BIOCHEMISTRY
including biophysical chemistry & molecular biology
Article

Biochemistry **2010,** *49,* 4085–4093 4085
DOI: 10.1021/bi1002844

Trema and *Parasponia* Hemoglobins Reveal Convergent Evolution of Oxygen Transport in Plants

Ryan Sturms, Smita Kakar, James Trent III, and Mark S. Hargrove*

Department of Biochemistry, Biophysics, and Molecular Biology, Iowa State University, Ames, Iowa 50011

Received February 25, 2010; Revised Manuscript Received April 2, 2010

ABSTRACT: All plants contain hemoglobins that fall into distinct phylogenetic classes. The subset of plants that carry out symbiotic nitrogen fixation expresses hemoglobins that scavenge and transport oxygen to bacterial symbiotes within root nodules. These "symbiotic" oxygen transport hemoglobins are distinct in structure and function from the nonoxygen transport ("nonsymbiotic") Hbs found in all plants. Hemoglobins found in two closely related plants present a paradox concerning hemoglobin structure and function. *Parasponia andersonii* is a nitrogen-fixing plant that expresses a symbiotic hemoglobin (ParaHb) characteristic of oxygen transport hemoglobins in having a pentacoordinate ferrous heme iron, moderate oxygen affinity, and a relatively rapid oxygen dissociation rate constant. A close relative that does not fix nitrogen, *Trema tomentosa*, expresses hemoglobin (TremaHb) sharing 93% amino acid identity to ParaHb, but its phylogeny predicts a typical nonsymbiotic hemoglobin with a hexacoordinate heme iron, high oxygen affinity, and slow oxygen dissociation rate constant. Here we characterize heme coordination and oxygen binding in TremaHb and ParaHb to investigate whether or not two hemoglobins with such high sequence similarity are actually so different in functional behavior. Our results indicate that the two proteins resemble nonsymbiotic hemoglobins in the ferric oxidation state and symbiotic hemoglobins in the ferrous oxidation state. They differ from each other only in oxygen affinity and oxygen dissociation rate constants, two factors key to their different functions. These results demonstrate distinct mechanisms for convergent evolution of oxygen transport in different phylogenetic classes of plant hemoglobins.

The history of hemoglobins (Hbs)[1] predates the photosynthetic oxygenation of earth (*1*−*3*). The "oxygen catastrophe" that occurred approximately 2 billion years ago greatly increased atmospheric oxygen, forcing organisms to avoid, tolerate, or exploit this change in their physiochemical environments. Thus, early Hbs probably protected cells from oxygen toxicity (*4*, *5*). As aerobic organisms grew larger and evolved more specialized tissues, their surface-to-volume ratios decreased, and passive oxygen diffusion became limiting. In response to this pressure, oxygen transport mechanisms evolved nearly 500 million years ago enabling organisms to grow to unprecedented size, complexity, and diversity (*2*). The modern day forms of these proteins are the hemocyanins in mollusks and arthropods, hemerythrins in marine worms, and oxygen transport Hbs in animals and plants. However, oxygen transport is certainly not the primordial or even the most common function of Hbs (*6*, *7*). Bacterial and yeast Hbs destroy toxic molecules like nitric oxide encountered in their environments (*8*), and animals contain specialized Hbs in neural and other tissues that are suggested to do the same (*9*−*11*). Although a few plant species contain oxygen transport Hbs, all plants contain Hbs unrelated to oxygen transport (*12*). The fact that the majority of Hbs do not function in oxygen transport suggests that the capacity for oxygen transport is a fairly recent development in the Hb evolutionary timeline.

A comparison of oxygen transport Hbs in plants and animals to the other Hbs present in the same organisms reveals distinct differences in structure and behavior (*13*). Oxygen transport Hbs are present in high millimolar concentrations, and their rate constants for oxygen release are relatively rapid (greater than 1 s^{-1}). Moreover, their association equilibrium constants are moderate, enabling them to bind oxygen when it is present, yet release it when needed. The heme groups in known oxygen transporters are "pentacoordinate" with an open binding site to the iron, characterized by a single histidine coordinating the "proximal" side of the heme, leaving the "distal" site open for reversible oxygen binding (Figure 1). The distal site often houses another histidine (called the "distal" histidine) that does not coordinate the heme iron but is in close proximity to and interacts with bound oxygen.

Hbs not involved in oxygen transport, including the "nonsymbiotic" (nsHbs) found in all plants, as well as neuroglobin (*14*−*16*) and cytoglobin (*17*, *18*) found in animals, have a second histidine reversibly coordinating the ligand binding site (Figure 1). While these proteins share globin folds, their heme active sites resemble that of cytochrome b_5. These Hbs are known as "hexacoordinate" Hbs (hxHbs), and their structures and chemistries are subjects of increasing attention due to potential roles in sensing and detoxifying nitric oxide and other environmental challenges.

It has been hypothesized that oxygen transport Hbs evolved from hxHbs independently in both plants and animals (*14*, *19*, *20*). In both cases, the chemical challenge was to express hemoglobin with stable pentacoordinate heme coordination. This is a difficult task to achieve because the change in spin state of the iron d-shell electrons upon histidine coordination is energetically very

*To whom correspondence should be addressed. Phone: 515-294-2616. E-mail: msh@iastate.edu. Fax: 515-294-0453.

[1]Abbreviations: Hbs, hemoglobins; hxHbs, hexacoordinate hemoglobins; TremaHb, *Trema tomentosa* hemoglobin; ParaHb, *Parasponia andersonii* hemoglobin; nsHb, nonsymbiotic hemoglobin; Lb, leghemoglobin; Lba, soybean leghemoglobin "a".

Published on Web 04/08/2010

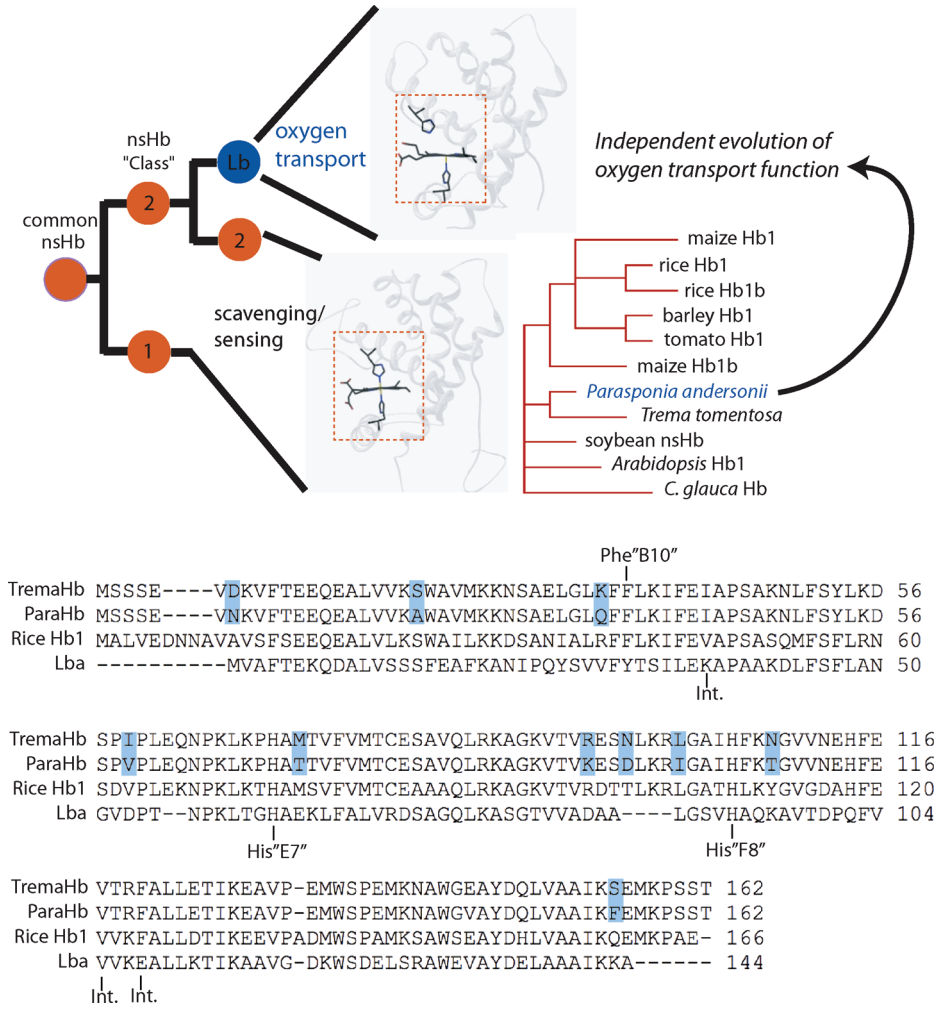

FIGURE 1: The phylogeny of oxygen transport hemoglobins in plants. Oxygen transport Hbs have evolved from two phylogenetic classes of nonsymbiotic Hbs (nsHbs). In each case, the oxygen transport proteins are pentacoordinate in the ferrous state (top inset structure), while the precursor nsHbs are hexacoordinate (bottom inset structure). The oxygen transport leghemoglobins (Lbs) evolved from "class 2" nonsymbiotic Hb (nsHbs), while *P. andersonii* is a class 1-derived oxygen transport Hb (ParaHb) that is 93% identical to the nsHb from *T. tomentosa*. The amino acid sequences for ParaHb, TremaHb, rice nsHb, and soybean Lba are shown at the bottom, with the 11 differences between ParaHb and TremaHb highlighted in blue. Also indicated on the sequences are the distal (E7) and proximal (F8) histidines, phenylalanine at position B10, and the positions of conserved dimer interface amino acids (Int.).

favorable (*21*−*23*), and holding a histidine near the heme iron without allowing it to bind presents a formidable thermodynamic challenge. Thus, an oxygen transport Hb must provide a protein scaffold that can offset this coordination energy in order to stabilize a pentacoordinate heme center.

The evolution of oxygen transport function in plant Hbs occurred more recently (around 200 million years ago (*20*, *24*−*26*)) than in animal Hbs, making them a useful system for investigating protein structural elements that are instrumental in this change of function. The phylogeny of plant Hbs can be divided into three general classes, two of which are known predecessors of oxygen transport globins (*12*). The familiar oxygen transport "leghemoglobins" (Lbs) common to the legume family evolved from "class 2" nsHbs and still share ~40% sequence identity with nsHbs (compared to less than 20% for red blood cell Hb and nonoxygen transport Hbs in animals) (*13*). Plant oxygen transport Hbs have also evolved independently and much more recently from "class 1" nsHbs (*19*, *24*, *25*) (Figure 1). This more recent event has left pairs of proteins that have different functions but share very similar primary structures. An extreme example is found in *Parasponia andersonii* (*27*) (a nonlegume which fixes N_2 in root nodules) and *Trema tomentosa* (*28*) (which does not fix N_2). Their Hbs are 93% identical (differing in only 11 positions with no primary sequence gaps), yet *P. andersonii* Hb (ParaHb) is a pentacoordinate oxygen transporter and *T. tomentosa* (TremaHb) is predicted to be a typical hexacoordinate nsHb (Figure 1).

ParaHb has been shown to be pentacoordinate in the ferrous oxidation state and to have rate and affinity constants for oxygen that are appropriate for transport (*29*, *30*). However, little is known about TremaHb or ferric ParaHb. The comparative experiments presented here were designed to test whether these proteins are truly as divergent in structure and chemistry as their physiological expression would suggest or whether their behavior mirrors the similarity of their sequence identity. The former result would reveal a surprising difference in physical behavior for two proteins sharing such high sequence identity, and the latter would suggest that pentacoordinate oxygen transporters could play the role of nsHbs and that hexacoordination *per se* is not an important structural feature for their physiological function.

EXPERIMENTAL PROCEDURES

Production of Proteins. Recombinant rice nsHb1 and soybean Lba were produced as described previously (*31*, *32*).

Codon-optimized cDNA for *P. andersonii* (GenBank number u27194) and *T. tomentosa* hemoglobins (GenBank number 1402313a) were synthesized by Epoch Biolabs using assembly PCR. These cDNAs were inserted into a pET28a plasmid for expression in the BL21 Star DE3 *Escherichia coli* strain. A second sequence for *T. tomentosa* hemoglobin (GenBank number y00296) was deposited more recently that differs from the former by lacking the conserved Val^{117} amino acid. Both Trema cDNAs were expressed in *E. coli*, but only the former (which included Val^{117}) produced soluble hemoglobin.

The BL21 Star DE3 host strain was grown in 2 L Erlenmeyer flasks that were inoculated using a 100 mL starter culture grown overnight to saturation. The expression medium used was 1 L of Terrific broth supplemented with 1 mL of 50 mg/mL kanamycin per flask. The flasks were cultured at 37 °C while being shaken for 18−20 h at 250 rpm without induction before being harvested by centrifugation (6000 rpm for 10 min). The collected cells were lysed by homogenization before being purified in a three-step process: (1) ammonium sulfate fractionation (60% and 90%), (2) immobilized metal affinity chromatography (BD TALON), and (3) size exclusion chromatography (HiPrep 26/60 Sephacryl S-100 high resolution). Collected fractions were dialyzed into 10 mM Tris buffer and concentrated using Amicon Millipore concentrators. Purification efficiency was measured by spectroscopic analysis of Soret/280 ratios. All absorbance spectra were measured using either a Cary-50 Bio or an Ocean Optics USB4000 spectrophotometer. Ferric protein was made by oxidizing each Hb with potassium ferricyanide followed by desalting over a G-25 column. Ferrous hemoglobins were generated by reducing ferric samples with sodium dithionite.

Kinetic Experiments. Flash photolysis and stopped-flow reactions were used to measure CO binding for all proteins as described previously (*33*, *34*). Oxygen association and dissociation rate constants were measured by flash photolysis and rapid mixing with CO, respectively (*35*). All kinetic traces were fit to exponential decays using Igor Pro. Calculation of rate constants for hexacoordination and CO binding used the method described by Smagghe et al. (*34*). Affinity constants for azide were measured using previously described methods (*36*).

Electrochemical and Quaternary Structure Analysis. Midpoint reduction potentials were measured by potentiometric titration using an apparatus described in detail previously (*37*). The biphasic reduction curve exhibited by ParaHb was evident under a range of conditions. This prompted our analysis of the oligomeric state of the ferric proteins by equilibrium analytical ultracentrifugation. This procedure followed one published earlier (*38*) with the exception that a newer model Beckman Coulter ProteomeLab XLA ultracentrifuge was used. Molecular mass was calculated from the linear portions of the plots in Figure 4 using eq 1, where M is molecular mass, r is the radial position of the sample, v is partial specific volume (fixed at 0.72 mL/g), ρ is solvent density (fixed at 0.9982 g/mL), the angular velocity ω = 3099 rads/s (29600 rpm), R = 8.31441 × 10^7 (g cm^2)/(s^2 K mol), and T was 293 K.

$$\ln(\text{Abs}) = \frac{M(1-v\rho)\omega^2}{2RT} r^2 \quad (1)$$

RESULTS

The experiments presented here are designed to measure three characteristics that distinguish the structure and reactivity of oxygen transport proteins from those of nsHbs. These characteristics are endogenous histidine coordination in the ferric oxidation state, endogenous histidine coordination in the ferrous oxidation state, and the kinetics of oxygen binding. NsHbs are hexacoordinate in both oxidation states, as described by the reaction (*33*):

$$\text{Hb}_{\text{hex}} \underset{k_{\text{H}}}{\overset{k_{-\text{H}}}{\leftrightarrow}} \text{Hb}_{\text{pent}} + \text{L} \underset{k_{\text{L}}}{\overset{k'_{\text{L}}}{\leftrightarrow}} \text{Hb}_{\text{L}} \quad (2)$$

In this equation, Hb_{hex} and Hb_{pent} are the hexacoordinate and pentacoordinate forms of the Hb, and the rate constants for distal histidine coordination (H) and exogenous ligand (L) binding are written at the top (for association) and bottom (for dissociation) of each step. The influence of distal histidine coordination on equilibrium binding affinity can be evaluated by the equation:

$$K_{\text{eff}} = \frac{K_{\text{L, pent}}}{1 + K_{\text{H}}} \quad (3)$$

Here $K_{L,pent}$ is k'_L/k_L (the affinity constant in the absence of the influence of histidine coordination), and K_H (k_H/k_{-H}) is the affinity constant for endogenous histidine coordination. Equation 3 predicts a decrease in affinity for exogenous ligand binding when histidine coordination is tight.

The rates of exogenous ligand binding can be influenced by histidine coordination as described by eq 4, which allows measurement of k_H and k_{-H} using appropriate ligands in the ferric and ferrous oxidation states (*33*):

$$k_{\text{obs}} = \frac{k_{-\text{H}} k'_{\text{L}}[\text{L}]}{k_{\text{H}} + k_{-\text{H}} + k'_{\text{L}}[\text{L}]} \quad (4)$$

Equation 4 predicts a limited rate of exogenous ligand binding when coordinated histidine dissociation is slow.

Coordination and Ligand Binding in the Ferric Oxidation State. A principal distinction between oxygen transport Hbs and nsHbs is hexacoordination in the latter, which is generally much stronger in the ferric than the ferrous oxidation state (*21*, *37*). Coordination state is evident from the visible region absorbance spectra in both oxidation states (*39*, *40*) as exemplified for hxHbs by rice nsHb and for pentacoordinate Hbs by soybean Lba (Figure 2). The prominent band at 529 nm and shoulder at 560 nm of rice nsHb are characteristic of a ferric, low-spin hemichrome heme center. In contrast, the larger degree of absorbance at 484 nm and the peak at 620 nm in the spectrum of Lba are characteristic charge-transfer bands found in high-spin, pentacoordinate ferric heme proteins. The absorbance spectra of recombinant ParaHb is (as shown by Appleby et al. (*19*) for the native protein) largely low spin (hexacoordinate) but with a measurable fraction of high-spin character evident from a minor 620 nm absorbance band. However, TremaHb is entirely low spin and functionally indistinguishable from rice nsHb.

To measure the impact of hexacoordination in ParaHb and TremaHb, equilibrium affinities for the ferric ligand, azide, were measured along with soybean Lba and rice nsHb as pentacoordinate and hexacoordinate controls, respectively. The binding curves for each are shown in Figure 2B. In these experiments, Lba binds azide stoichiometrically with an affinity constant precluding measurement at this protein concentration (5 μM). The other three proteins, however, bind azide with much lower affinities (each constant is on the order of 3 mM), as would be expected from eq 3 for hxHbs with higher values of K_H. The data in Figure 2 reveal that TremaHb and ParaHb are predominately

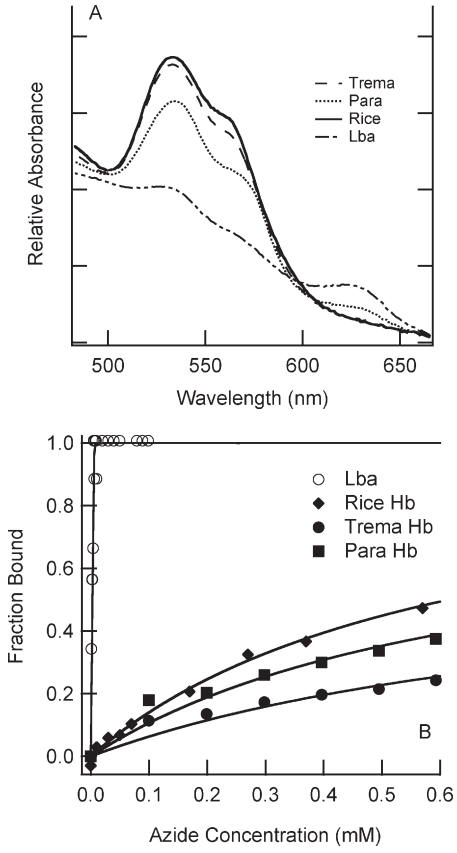

FIGURE 2: Coordination and ligand binding in the ferric oxidation state. (A) Absorbance spectra of oxidized TremaHb and rice nsHb are typical of hexacoordinate, low-spin ferric hemoglobins. That of soybean Lba is characteristic of a high-spin, pentacoordinate complex. The ParaHb spectrum represents a mixture of high- and low-spin heme. (B) Azide binding to each protein shows that TremaHb, ParaHb, and rice nsHb bind with much lower affinity than soybean Lba, indicating competition from histidine coordination in the former three Hbs.

hexacoordinate in the ferric oxidation states. Thus, they share similarity to nsHbs rather than Lbs for this property.

Coordination and Ligand Binding in the Ferrous Oxidation State. Heme coordination in the ferrous oxidation state is evident from splitting of the visible bands seen in low-spin complexes. Bishistidyl ferrous heme coordination results in prominent peaks at 528 and 556 nm that resemble the visible spectrum of cytochrome b_5. Figure 3A shows the absorbance spectra of rice nsHb, ParaHb, and TremaHb in this region. To provide a reference for the degree of histidine coordination in these proteins, absorbance spectra for human neuroglobin (Ngb) (fraction of coordination ~1) and Lba (fraction of coordination ~0) are included. The ratio of absorbance at 555 nm to that at 540 nm has been shown to reflect the fraction of hexacoordination (*34*) (Figure 3B). The line in Figure 3B was established empirically for this relationship (*34*). These data estimate that both TremaHb and ParaHb are fractionally coordinated at a ratio less than 0.2.

The low degree of ferrous hexacoordination in TremaHb and ParaHb is supported by the kinetics of CO binding. Figure 3C demonstrates the effect of histidine coordination in rice nsHb, showing CO binding time courses for [CO] ranging from 12 to 500 μM. In each case (Figure 3C−E), the *y*-axes are normalized to absorbance change expected for the reaction. The time courses for rice nsHb are relatively slow, show appreciable loss of amplitude only at the highest [CO], and coalesce to a concentration-independent rate constant as [CO] is raised (Figure 3F). These phenomena are characteristic of hexacoordination as exhibited by rice nsHb, described by eq 4 when K_H is appreciable, and k_H and k_{-H} are on the order of k'_{CO} (*34*). In contrast, CO binding to ParaHb (Figure 3D) and TremaHb (Figure 3E) is much faster, and the majority of the absorbance change is lost in the dead time of the reaction at even moderate [CO] (the maximum [CO] in Figure 3D,E is 125 μM). Furthermore, there is a linear relationship between the observed rate constants and [CO]. Lba is not included in Figure 3 because its rate of CO binding is too fast for analysis by rapid mixing. These characteristics are common to bimolecular CO binding in the absence of appreciable K_H and demonstrate that ParaHb and TremaHb resemble Lba and other pentacoordinate Hbs in the ferrous oxidation state.

Values of k_{-H2} can be estimated from the data in Figure 3 by examination of the rate constant for binding to the slower fraction (~15%) at the highest [CO] (*34*). These values are reported in Table 1 along with the bimolecular rate constants for CO association. Knowing k_{-H2} and K_H allows an estimation of the rate constant for histidine binding (k_{H2}), which is also reported in Table 1.

Electrochemical Analysis. Binding of the distal histidine to form a bishistidyl heme complex is generally favored more in the ferric oxidation state than the ferrous (*21*). The data above suggest that hexacoordination is significant in ferric TremaHb and ParaHb but not in the ferrous forms of each protein. As is the case for other hexacoordinate heme proteins, this should result in midpoint reduction potentials that are more negative than for Hbs that are strictly pentacoordinate (*37*). To test this hypothesis, potentiometric titration was used to measure the midpoint reduction potentials for ParaHb and TremaHb compared to Lba and rice nsHb. As demonstrated previously (*37*), the midpoint reduction potential for rice nsHb is −132 mV (versus SHE), and that of Lba is +13 mV. As expected for histidine coordination preferentially in the ferric oxidation state, the midpoint reduction potential for TremaHb is −138 mV. Surprisingly, the ParaHb redox titration is biphasic, with 50% of the population having a midpoint reduction potential of 0 mV and 50% at −150 mV.

There are many ways in which heme coordination by histidine can influence midpoint reduction potentials in hxHbs. For example, differential coordination strength in the ferric and ferrous oxidation states leads to lower reduction potentials in all hxHbs due to tighter binding in the ferric oxidation state (*37*). However, none of the known reactions can account for biphasic equilibrium redox titration curves, as they are all at rapid exchange on the time scale of a potentiometric titration and would result in an observed average behavior. A mechanistic explanation for biphasic redox titration requires the assumption of dissimilar heme sites that are not interconverting. Alternatively, but less likely, the same result would be expected from a change in coordination state slower than the time scale (hours) of the experiment.

Two dissimilar heme sites are difficult to rationalize with a monomeric Hb (like Lba). Likewise, rice nsHb has a dissociation equilibrium constant for dimerization of 86 μM (*38*), leaving it mostly monomeric in our experiments (5 μM in Hb concentration). However, the original purification of native ParaHb reported it as a "readily dissociable dimer" (*19*). Our potentiometric titration results would be easier to explain if in fact ParaHb had a much lower K_D for dimerization. This possibility

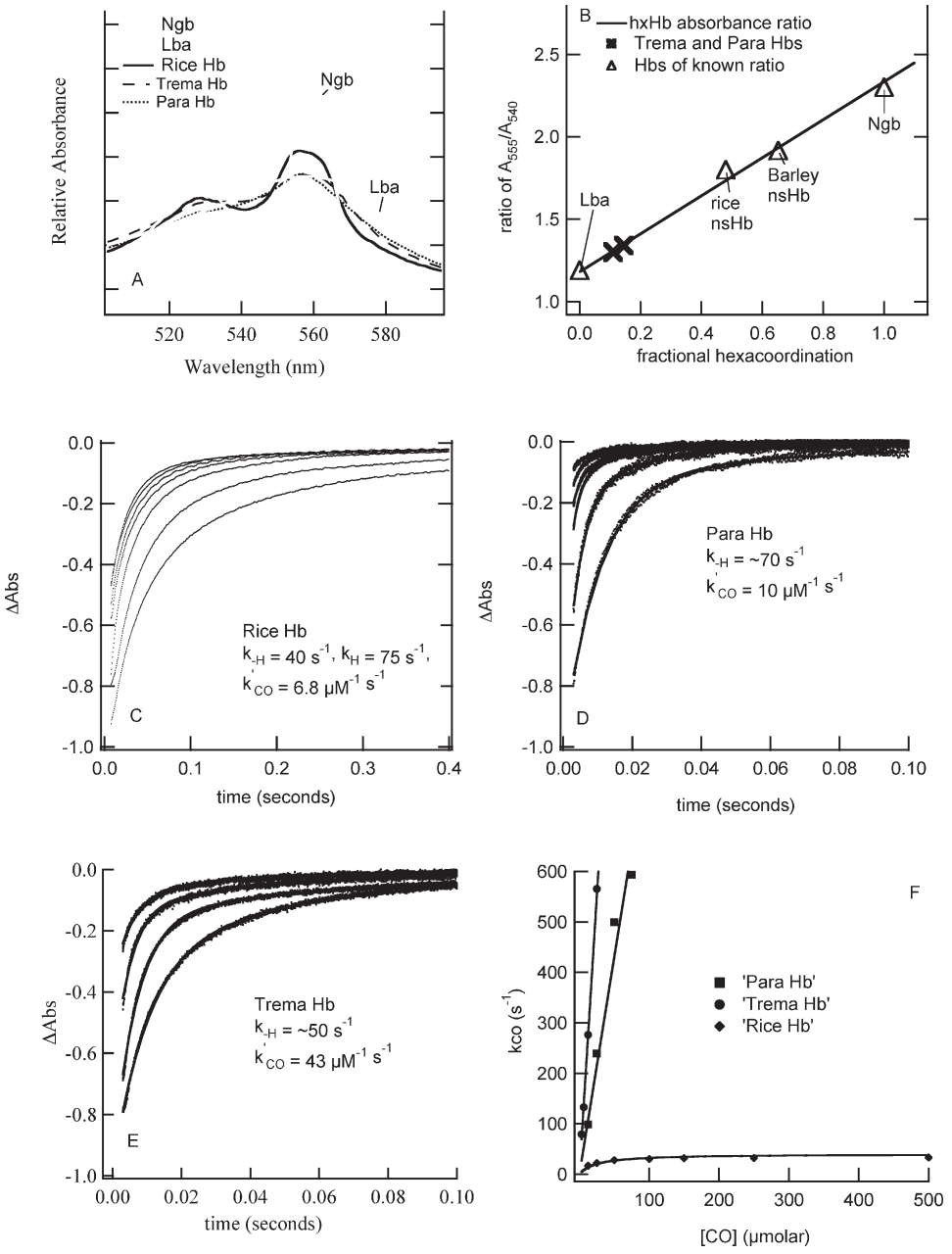

FIGURE 3: Coordination and ligand binding in the ferrous oxidation state. (A) Absorbance spectra of each Hb in the ferrous oxidation state are compared to human neuroglobin (Ngb) which is completely hexacoordinate in ferrous oxidation state. (B) Empirical quantification of the ratio of absorbance at 555 nm/540 nm indicates that ParaHb and TremaHb have a fraction of histidine coordination of < 0.2. (C−E) Time courses for CO binding to each Hb at varying [CO] reveal the fraction of hexacoordinate Hb and the rate constants for histidine binding and dissociation. (F) The concentration dependence of the observed rate constant for the fast phase of CO binding to each Hb shows that ParaHb and TremaHb are predominately pentacoordinate, and rice nsHb has an appreciable fraction of hexacoordinate heme.

was measured using equilibrium analytical ultracentrifugation to analyze the quaternary structure of ferric ParaHb and TremaHb (Figure 4B). In this experiment, rice nsHb, TremaHb, and ParaHb were analyzed at a concentration of 5 μM (in heme). At this concentration, rice nsHb is mainly monomeric and has an apparent molecular mass of 17.3 kDa. However, at the same concentration, TremaHb and ParaHb have molecular masses of 32.8 and 31 kDa, respectively, indicating that they are largely dimeric even at this low concentration. From these data and eq 1, it can be estimated that K_D values for dimerization for these proteins are no greater than 1 μM. These results show that ParaHb is in fact dimeric in our potentiometric titration experiments and make asymmetric heme sites a plausible cause of the biphasic redox titration curve observed for this protein.

Table 1

	ferrous ligand binding and hexacoordination values			
	$k'_{CO,pent}$ (μM^{-1} s^{-1})	k_{H2} (s^{-1})	k_{-H2} (s^{-1})	K_{H2}
Lba	13			~0
rice Hb	6.8	75	40	1.9
ParaHb	10	~7[c]	~70[b]	~0.1[a]
TremaHb	43	~5[c]	~50[b]	~0.1[a]

[a]Estimated from the ferrous absorption spectrum and the amplitude of CO binding at high [CO]. [b]k_{obs} at high [CO]. [c]Estimated from K_H and k_{-H}.

Oxygen Binding. Our results so far suggest that in the ferric oxidation state TremaHb and ParaHb resemble nsHbs, but in the

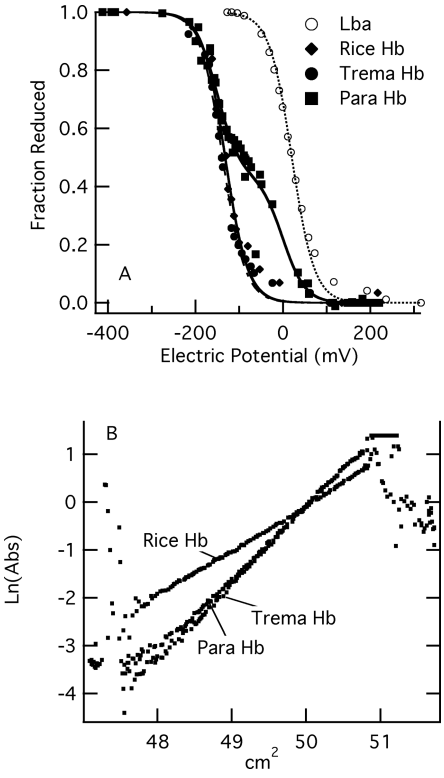

FIGURE 4: Potentiometric titrations and equilibrium analytical ultracentrifugation analysis. (A) Nernst plots of potentiometric titrations were used to measure the ferrous/ferric redox potential for each Hb. (B) Each ferric Hb was analyzed at 5 μM by equilibrium analytical ultracentrifugation monitored at 410 nm. The slopes of the plots for ParaHb and TremaHb indicate a tighter dimer than that observed for rice nsHb.

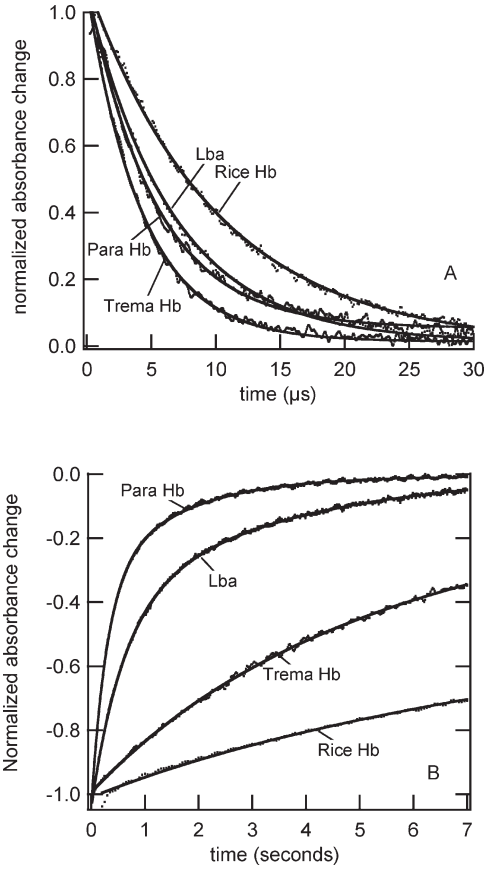

FIGURE 5: Kinetics of oxygen binding to ParaHb and TremaHb. (A) Time courses for oxygen association and (B) dissociation for ParaHb, TremaHb, rice nsHb, and soybean Lba in air. The dissociation curves in (B) were measured against displacement by 1 mM CO.

ferrous state, they both share more similarity with pentacoordinate oxygen transporters like Lba. Our final test to distinguish between oxygen transport Hbs and typical hexacoordinate Hbs is a measurement of oxygen affinity and kinetics. ParaHb has kinetic and affinity constants for oxygen similar to Lbs (*12*, *29*). To compare these results with those of TremaHb, Figure 5A shows oxygen binding (following flash photolysis), and Figure 5B shows time courses for oxygen dissociation for both proteins (again with Lba and rice nsHb as controls). The association rate constants for TremaHb and ParaHb are similar (210 and 170 μM^{-1} s^{-1}, respectively). However, the oxygen dissociation rate constants are quite distinct at 0.38 and 12 s^{-1}, respectively. This 30-fold difference in respective oxygen dissociation rate constants is a clear functional distinction between ParaHb and TremaHb. The oxygen dissociation rate constant for TremaHb (0.38 s^{-1}) groups it with the nsHbs, and the rate constant for Para Hb (12 s^{-1}) is consistent with the oxygen transport function of the Lbs (Table 2).

Table 2

protein	$k'_{O_2,pent}$ (μM^{-1} s^{-1})	k_{O_2} (s^{-1})	$K_{O_2,pent}$ (μM^{-1})	K_{O_2} (μM^{-1})
rice Hb1	60	0.038	1600	540
soybean Lba	130	5.6	23	23
T. tomentosa	210	0.38	550	500
P. andersonii (native)	165	15	11	11
P. andersonii (recombinant)	170	12	14	13

DISCUSSION

The rationale for this investigation was the high level of sequence similarity between ParaHb, a typical plant oxygen transport protein, and TremaHb, which is predicted to be distinct from known oxygen transporters in heme coordination and oxygen binding kinetics. There were two possible outcomes anticipated. The first was that TremaHb could have been identical to ParaHb in its behavior, implying that the physical differences between nsHbs and oxygen transport Hbs are not necessary for nsHb function, which would mean that oxygen transporters could possibly function as nsHbs. The second possible outcome was a difference between the two proteins, demonstrating that a surprisingly small number of amino acid changes are responsible for a large shift in structure and function. With respect to oxygen binding, our results support the latter conclusion. The oxygen affinity and binding kinetics of TremaHb are not suitable for oxygen transport and completely in line with class 1 nsHbs. However, with respect to hexacoordination, the conclusions are mixed; both Hbs are predominately hexacoordinate in the ferric oxidation state and mostly pentacoordinate in the ferrous oxidation state. They are distinct from other nsHbs in having ~20-fold (class 1) or ~800-fold (class 2) lower affinities for ferrous distal histidine coordination. Furthermore, in contrast to both Lbs and class 1 nsHbs, ParaHb and TremaHb are tightly associated dimers. The implications of these results to the evolution of oxygen transport Hbs are discussed below.

Independent Evolution of Oxygen Transport Hbs in Plants: Class 1 versus Class 2 Oxygen Transport Hemoglobins.

Table 3

protein	k_{H2} (s^{-1})	k_{-H2} (s^{-1})	K_{H2}	$k'_{O_2,pent}$ ($\mu M^{-1} s^{-1}$)	k_{O_2} (s^{-1})	$K_{O_2,pent}$ (μM^{-1})	K_{O_2} (μM^{-1})
class 1 nsHbs	130	75	1.7	67	0.14	1200	410
rice Hb E7L				620	51	12	12
class 2 nsHbs	1500	25	84	76	1.1	260	2.9
plant oxygen transporters				230	13	20	20
Lba E7V				400	24	17	17

The two phylogenetic classes of nsHbs that have given rise to oxygen transport globins have distinct physical attributes, including the degree of hexacoordination found in each and their affinity constants for oxygen (Table 3) (*12*). In contrast, ParaHb and Lbs (which evolved from class 1 and class 2 nsHbs, respectively) are similar in their affinities for oxygen, and both lack significant histidine coordination in the ferrous oxidation state. The convergence of similar oxygen transport globins from dissimilar starting points required different molecular changes in each class of nsHb. In an effort to compare the molecular mechanisms that lead to the development of plant oxygen transport globins, average values for the rate and affinity constants for ferrous hexacoordination and oxygen binding for each nsHb class are provided in Table 3 along with rate and affinity constants for oxygen binding to the plant oxygen transport Hbs (taken from Smagghe et al. (*12*)).

If we choose to define the requirements of an oxygen transport Hb based solely on affinity and kinetics of oxygen binding, class 2 nsHbs are not far off the mark. With equilibrium constants averaging 3 μM^{-1} and dissociation rate constants averaging 1.1 s^{-1}, they would require only slight modification to attain the values shared by the Lbs. On the other hand, class 1 nsHbs would have to significantly lower their affinity for oxygen (by ~20-fold) and increase their oxygen dissociation rate constants (~10-fold). In addition to these changes is the apparent requirement of a pentacoordinate ferrous heme, based on the knowledge that all observed oxygen transporter Hbs are pentacoordinate in this oxidation state.

One possibility for overcoming the challenges of designing affinity, kinetics, and coordination is to change the distal histidine to an amino acid that cannot coordinate the heme iron. In fact, the mutant protein E7L of rice nsHb (in which the distal histidine is replaced by leucine) meets all of these requirements for oxygen transport (*41*) (Table 3). Likewise, histidine substitution mutations in soybean Lba are well suited for oxygen transport based on these criteria (*35*) (Table 3). However, all oxygen transport Hbs in plants (and in nearly all other organisms) not only are pentacoordinate but also contain histidine at position E7 near the ligand binding site. When considering the constraints of pentacoordinate ferrous heme and a nearby distal histidine, the act of converting both classes of nsHbs to oxygen transporters involves reducing the oxygen affinity values presented in Table 3 for class 1 and class 2 nsHbs ($K_{O_2,pent}$) to ~20 μM^{-1}. The oxygen affinities can be lowered by increasing the oxygen dissociation rate constant by ~90- and ~12-fold for class 1 and 2 nsHbs, respectively.

The molecular details resulting in the changes in oxygen dissociation rate constants are still unclear, though some hints are provided from biophysical studies of Lbs and nsHbs. Oxygen release can be controlled by hydrogen bonding with the distal histidine (*42*), by the nature of the proximal histidine−heme bond (*43*−*45*), and by control of geminate rebinding through cavities and tunnels in the protein matrix surrounding the heme (*46*, *47*). Previous research indicates that the distal histidine in class 2 nsHbs hydrogen bonds with bound oxygen (*12*), but the distal histidine present in soybean Lba does not form this same hydrogen bond (*31*, *35*). This suggests that the evolution of oxygen transport in class 2 Hbs resulted, at least in part, from the loss of oxygen stabilization by the distal histidine. However, until other class 2 nsHbs and Lbs are examined, this conclusion is tentative because of potentially different mechanisms for regulating oxygen affinity in other Lbs (*30*, *48*).

It is also known that class 1 nsHbs use a hydrogen bond to stabilize bound oxygen (*49*, *50*). Whether loss of this hydrogen bond causes the decrease in oxygen affinity in ParaHb has not been addressed but could be tested by analysis of ParaHb and TremaHb distal His mutant proteins. If the loss of this hydrogen bond were key to modulating oxygen affinity, it would be expected that distal His mutation in TremaHb would increase the oxygen dissociation rate constant, but that in ParaHb would not. However, a comparison of the amino acid sequences of these proteins reveals no obvious suspects that might influence oxygen dissociation rate constants between the two, or that would suggest a mechanism for regulating oxygen affinity (Figure 1). Both have Phe at position B10 (*36*), an apolar side chain at position F7 (*45*, *51*), and there are no substitutions predicted to be closer than ~10 Å to the distal heme pocket. Thus, a molecular explanation for the nearly 50-fold difference in oxygen affinity between ParaHb and TremaHb will require a detailed study of the structures of these Hbs and the behavior of key mutant proteins derived from each.

Why Are Oxygen Transport Hbs Pentacoordinate and Why Do They Retain a Distal Histidine? It has been proposed that oxygen transport Hbs evolved from hexacoordinate hemoglobins (hxHbs) in both plants and animals (*19*, *20*, *52*). In both cases, the functions of the precursor hxHbs are not yet clear, and the necessity of hexacoordination is accordingly unknown (*12*, *53*). The oxygen transport Hbs that evolved from them share similar features of pentacoordinate ferrous heme, relatively rapid oxygen dissociation, and in nearly all cases a distal histidine. The few exceptions among known oxygen transporters have substitutions of glutamine, which is capable of electrostatic interactions with ligands similar to but somewhat weaker than histidine (*54*−*56*). The requirement of a pentacoordinate ferrous heme is probably due to the effect of hexacoordination on heme oxidation, as it has been shown that both plant and animal hxHbs oxidize significantly faster than oxygen transport Hbs (*15*, *36*). For example, a bishistidyl myoglobin mutant protein oxidizes much more rapidly than the wild-type protein (*57*). The reason for this could be due to the ability of the bishistidyl heme center to more rapidly transfer electrons (*58*) or to the more negative reduction potentials that accompany disproportionately strong ferric distal histidine coordination (*15*, *37*).

The requirement for a distal histidine arises from the need for stabilization of bound oxygen (in some Hbs), ligand discrimination, and slowing of heme oxidation and subsequent hemin dissociation (*59*, *60*). The examples given above of the His E7L mutant proteins of rice nsHb and soybean Lba have appropriate kinetic and equilibrium constants for oxygen transport, but they are much poorer than their respective wild-type proteins in discriminating for oxygen against other potential ligands like carbon monoxide (*41*). Likewise, replacement of the distal histidine in most Hbs increases heme oxidation due to lower

oxygen affinity and increased solvent access to the heme pocket (*42*, *61*). Thus, oxygen transport Hbs require that histidine be located precariously near the ligand binding site but not so near as to coordinate the ferrous heme iron. This requirement of the cognate globin reveals that the architecture of oxygen transport proteins is a delicate balance of structure and coordination that is highlighted in comparison to their hxHb evolutionary precursors.

REFERENCES

1. Hardison, R. C. (1996) A brief history of hemoglobins: plant, animal, protist, and bacteria. *Proc. Natl. Acad. Sci. U.S.A. 93*, 5675–5679.
2. Hardison, R. C. (1999) The evolution of hemoglobins. *Am. Sci. 87*, 126–133.
3. Hardison, R. C. (1998) Hemoglobins from bacteria to man: evolution of different patterns of gene expression. *J. Exp. Bot. 201*, 1099–1117.
4. Raymond, J., and Segre, D. (2006) The effect of oxygen on biochemical networks and the evolution of complex life. *Science 311*, 1764–1767.
5. Falkowski, P. (2006) Tracing oxygen's imprint on earth's metabolic evolution. *Science 311*, 1724–1725.
6. Hankeln, T., Ebner, B., Fuchs, C., Gerlach, F., Haberkamp, M., Laufs, T. L., Roesner, A., Schmidt, M., Weich, B., Wystub, S., Saaler-Reinhardt, S., Reuss, S., Bolognesi, M., De Sanctis, D., Marden, M. C., Kiger, L., Moens, L., Dewilde, S., Nevo, E., Avivi, A., Weber, R. E., Fago, A., and Burmester, T. (2005) Neuroglobin and cytoglobin in search of their role in the vertebrate globin family. *J. Inorg. Biochem. 99*, 110–119.
7. Wittenberg, J. B., Wittenberg, B. A., and Guertin, M. (2002) Truncated hemoglobins: a new family of hemoglobins widely distributed in bacteria, unicellular eukaryotes, and plants. *J. Biol. Chem. 277*, 871–874.
8. Gardner, P. R., Gardner, A. M., Martin, L. A., and Salzman, A. L. (1998) Nitric oxide dioxygenase: an enzymatic function for flavohemoglobin. *Proc. Natl. Acad. Sci. U.S.A. 95*, 10378–10383.
9. Sun, Y., Jin, K., Mao, X., Zhu, Y., and Greenberg, D. A. (2001) Neuroglobin is up-regulated by and protects neurons from hypoxic-ischemia injury. *Proc. Natl. Acad. Sci. U.S.A. 98*, 15306–15311.
10. Sun, Y., Jin, K., Peel, A., Mao, X. O., Xie, L., and Greenberg, D. A. (2003) Neuroglobin protects the brain from experimental stroke invivo. *Proc. Natl. Acad. Sci. U.S.A. 100*, 3497–3500.
11. Khan, A. A., Wang, Y., Sun, Y., Mao, X. O., Xie, L., Miles, E., Graboski, J., Chen, S., Ellerby, L. M., Jin, K., and Greenberg, D. A. (2006) Neuroglobin-overexpressing transgenic mice are resistant to cerebral and myocardial ischemia. *Proc. Natl. Acad. Sci. U.S.A. 103*, 17944–17948.
12. Smagghe, B. J., Hoy, J. A., Percifield, R., Kundu, S., Hargrove, M. S., Sarath, G., Hilbert, J. L., Watts, R. A., Dennis, E. S., Peacock, W. J., Dewilde, S., Moens, L., Blouin, G. C., Olson, J. S., and Appleby, C. A. (2009) Review: Correlations between oxygen affinity and sequence classifications of plant hemoglobins. *Biopolymers 91*, 1083–1096.
13. Kundu, S., Trent, J. T., III, and Hargrove, M. S. (2003) Plants, humans, and hemoglobins. *Trends Plant Sci. 8*, 387–393.
14. Burmester, T., Welch, B., Reinhardt, S., and Hankeln, T. (2000) A vertebrate globin expressed in the brain. *Nature 407*, 520–523.
15. Dewilde, S., Kiger, L., Burmester, T., Hankeln, T., Baudin-Creuza, V., Aerts, T., Marden, M., Caubergs, R., and Moens, L. (2001) Biochemical characterization and ligand-binding properties of neuroglobin, a novel member of the globin family. *J. Biol. Chem. 276*, 38949–38955.
16. Trent, J. T., III., Watts, R. A., and Hargrove, M. S. (2001) Human neuroglobin, a hexacoordinate hemoglobin that reversibly binds oxygen. *J. Biol. Chem. 276*, 30106–30110.
17. Burmester, T., Ebner, B., Weich, B., and Hankeln, T. (2002) Cytoglobin: a novel globin type ubiquitously expressed in vertebrate tissues. *Mol. Biol. Evol. 19*, 416–421.
18. Trent, J. T., III., and Hargrove, M. S. (2002) A ubiquitously expressed human hexacoordinate hemoglobin. *J. Biol. Chem. 277*, 19538–19545.
19. Appleby, C. A., Tjepkema, J. D., and Trinick, M. J. (1983) Hemoglobin in a nonleguminous plant, *Parasponia:* possible genetic origin and function in nitrogen fixation. *Science 220*, 951–953.
20. Trevaskis, B., Watts, R. A., Andersson, C. R., Llewellyn, D. J., Hargrove, M. S., Olson, J. S., Dennis, E. S., and Peacock, W. J. (1997) Two hemoglobin genes in *Arabidopsis thaliana*: the evolutionary origins of leghemoglobins. *Proc. Natl. Acad. Sci. U.S.A. 94*, 12230–12234.
21. Cowley, A. B., Kennedy, M. L., Silchenko, S., Lukat-Rodgers, G. S., Rodgers, K. R., and Benson, D. R. (2006) Insight into heme protein redox potential control and functional aspects of six-coordinate ligand-sensing heme proteins from studies of synthetic heme peptides. *Inorg. Chem. 45*, 9985–10001.
22. Nesset, M., Shokhirev, N., Enemark, P., Jacobson, S., and Walker, F. (1996) Models of the cytochromes. Redox properties and thermodynamic stabilities of complexes of "hindered" iron(III) and iron(II) tetraphenylporphyrinates with substituted pyridines and imidazoles. *Inorg. Chem. 35*, 5188–5200.
23. Safo, M. K., Nesset, M. J. M., Walker, F. A., Debrunner, P. G., and Scheidt, W. R. (1997) Models of the cytochromes. Axial ligand orientation and complex stability in iron(II) porphyrinates: the case of the noninteracting d orbitals. *J. Am. Chem. Soc. 119*, 9438–9448.
24. Guldner, E., Desmariais, E., Galtier, N., and Godelle, B. (2004) Molecular evolution of plant haemoglobin: two haemoglobin genes in nymphaeaceae *Euryale ferox*. *J. Evol. Biol. 59*, 48–54.
25. Guldner, E., Godelle, B., and Galteir, N. (2004) Molecular adaptation in plant hemoglobin, a duplicated gene involved in plant−bacteria symbiosis. *J. Mol. Evol. 59*, 416–425.
26. Hunt, P. W., Watts, R. A., Trevaskis, B., Llewellyn, D. J., Burnell, J., Dennis, E. S., and Peacock, W. J. (2001) Expression and evolution of functionally distinct haemoglobin genes in plants. *Plant Mol. Biol. 47*, 677–692.
27. Kortt, A., Trinick, M., and Appleby, C. (1988) Amino acid sequences of hemoglobins I and II from root nodules of the non-leguminous *Parasponia rigida-rhizobium* symbiosis, and a correction of the sequence of hemoglobin I from Parasponia andersonii. *Eur. J. Biochem. 175*, 141–149.
28. Bogusz, D., Appleby, C. A., Landsmann, J., Dennis, E. S., Trinick, M. J., and Peacock, W. J. (1988) Functioning haemoglobin genes in non-nodulating plants. *Nature 331*, 178–180.
29. Wittenberg, J. B., Wittenberg, B. A., Gibson, Q. H., Trinick, M. J., and Appleby, C. A. (1986) The kinetics of the reactions of *Parasponia andersonii* hemoglobin with oxygen, carbon monoxide, and nitric oxide. *J. Biol. Chem. 261*, 13624–13631.
30. Gibson, Q. H., Wittenberg, J. B., Wittenberg, B. A., Bogusz, D., and Appleby, C. A. (1989) The kinetics of ligand binding to plant hemoglobins: structural implications. *J. Biol. Chem. 264*, 100–107.
31. Hargrove, M. S., Barry, J. K., Brucker, E. A., Berry, M. B., Phillips, G. N., Jr., Olson, J. S., Arredondo-Peter, R., Dean, J. M., Klucas, R. V., and Sarath, G. (1997) Characterization of recombinant soybean leghemoglobin a and apolar distal histidine mutants. *J. Mol. Biol. 266*, 1032–1042.
32. Hargrove, M., Brucker, E., Stec, B., Sarath, G., Arredondo-Peter, R., Klucas, R., Olson, J., and Phillips, G. (2000) Crystal structure of a nonsymbiotic plant hemoglobin. *Struct. Folding Des. 8*, 1005–1014.
33. Smagghe, B. J., Halder, P., and Hargrove, M. S. (2008) Measurement of distal histidine coordination equilibrium and kinetics in hexacoordinate hemoglobins. *Methods Enzymol. 436*, 359–378.
34. Smagghe, B. J., Sarath, G., Ross, E., Hilbert, J. L., and Hargrove, M. S. (2006) Slow ligand binding kinetics dominate ferrous hexacoordinate hemoglobin reactivities and reveal differences between plants and other species. *Biochemistry 45*, 561–570.
35. Kundu, S., and Hargrove, M. S. (2003) Distal heme pocket regulation of ligand binding and stability in soybean leghemoglobin. *Proteins 50*, 239–248.
36. Smagghe, B. J., Kundu, S., Hoy, J. A., Halder, P., Weiland, T. R., Savage, A., Venugopal, A., Goodman, M., Premer, S., and Hargrove, M. S. (2006) Role of phenylalanine B10 in plant nonsymbiotic hemoglobins. *Biochemistry 45*, 9735–9745.
37. Halder, P., Trent, J. T., III., and Hargrove, M. S. (2007) The influence of the protein matrix on histidine ligation in ferric and ferrous hexacoordinate hemoglobins. *Proteins: Struct., Funct., Bioinf. 66*, 172–182.
38. Goodman, M. D., and Hargrove, M. S. (2001) Quaternary structure of rice nonsymbiotic hemoglobin. *J. Biol. Chem. 276*, 6834–6839.
39. Appleby, C. A. (1969) The separation and properties of low-spin (haemochrome) and native, high-spin forms of leghaemoglobin from soybean nodule extracts. *Biochim. Biophys. Acta 189*, 267–279.
40. Yonetani, T., Iizuka, T., and Waterman, M. R. (1971) Studies on modified hemoglobins. 3. Spin states of ferric hemoglobin, semihemoglobin, and isolated subunit chains. *J. Biol. Chem. 246*, 7683–7689.
41. Arredondo-Peter, R., Hargrove, M. S., Sarath, G., Moran, J. F., Lohrman, J., Olson, J. S., and Klucas, R. V. (1997) Rice hemoglobins. Gene cloning, analysis, and O_2-binding kinetics of a recombinant protein synthesized in *Escherichia coli*. *Plant Physiol. 115*, 1259–1266.

42. Springer, B. A., Egeberg, K. D., Sligar, S. G., Rohlfs, R. J., Mathews, A. J., and Olson, J. S. (1989) Discrimination between oxygen and carbon monoxide and inhibition of autooxidation by myoglobin. Site-directed mutagenesis of the distal histidine. *J. Biol. Chem. 264*, 3057–3060.
43. Perutz, M. F. (1970) Stereochemistry of cooperative effects in haemoglobin. *Nature 228*, 726–739.
44. Smerdon, S. J., Krzywda, S., Wilkinson, A. J., Brantley, R. E., Jr., Carver, T. E., Hargrove, M. S., and Olson, J. S. (1993) Serine92 (F7) contributes to the control of heme reactivity and stability in myoglobin. *Biochemistry 32*, 5132–5138.
45. Kundu, S., Snyder, B., Das, K., Chowdhury, P., Park, J., Petrich, J. W., and Hargrove, M. S. (2002) The leghemoglobin proximal heme pocket directs oxygen dissociation and stabilizes bound heme. *Proteins 46*, 268–277.
46. Scott, E. E., Gibson, Q. H., and Olson, J. S. (2001) Mapping the pathways for O2 entry into and exit from myoglobin. *J. Biol. Chem. 276*, 5177–5188.
47. Salter, M. D., Nienhaus, K., Nienhaus, G. U., Dewilde, S., Moens, L., Pesce, A., Nardini, M., Bolognesi, M., and Olson, J. S. (2008) The apolar channel in *Cerebratulus lacteus* hemoglobin is the route for O2 entry and exit. *J. Biol. Chem. 283*, 35689–35702.
48. Kundu, S., Blouin, G., Premer, S., Sarath, G., Olson, J., and Hargrove, M. (2004) TyrB10 inhibits stabilization of bound oxygen in soybean leghemoglobin. *Biochemistry 43*, 6241–6252.
49. Arredondo-Peter, R., Moran, J. F., Sarath, G., Luan, P., and Klucas, R. V. (1997) Molecular cloning of the cowpea leghemoglobin II gene and expression of its cDNA in *Escherichia coli*. Purification and characterization of the recombinant protein. *Plant Physiol. 114*, 493–500.
50. Watts, R. (1999) Characterisation of non-symbiotic haemoglobins from dicotyledonous plants, Ph.D. Thesis, Division of Biochemistry and Molecular Biology, Australian National University.
51. Smerdon, S. J., Dodson, G. G., Wilkinson, A. J., Gibson, Q. H., Blackmore, R. S., Carver, T. E., and Olson, J. S. (1991) Distal pocket polarity in ligand binding to myoglobin: structural and functional characterization of a threonine^{68} (E11) mutant. *Biochemistry 30*, 6252–6260.
52. Burmester, T., Weich, B., Reinhardt, S., and Hankeln, T. (2000) A vertebrate globin expressed in the brain. *Nature 407*, 520–523.
53. Hankeln, T., Ebner, B., Fuchs, C., Gerlach, F., Haberkamp, M., Laufs, T., Roesner, A., Schmidt, M., Weich, B., Wystub, S., Saaler-Reinhardt, S., Reuss, S., Bolognesi, M., De Sanctis, D., Marden, M., Kiger, L., Moens, L., Dewilde, S., Nevo, E., Avivi, A., Weber, R., Fago, A., and Burmester, T. (2005) Neuroglobin and cytoglobin in search of their role in the vertebrate globin family. *J. Inorg. Biochem. 99*, 110–119.
54. Rohlfs, R. J., Mathews, A. J., Carver, T. E., Olson, J. S., Springer, B. A., Egeberg, K. D., and Sligar, S. G. (1990) The effects of amino acid substitution at position E7 (residue 64) on the kinetics of ligand binding to sperm whale myoglobin. *J. Biol. Chem. 265*, 3168–3176.
55. Olson, J. S., and Phillips, G. N., Jr. (1997) Myoglobin discriminates between O_2, NO, and CO by electrostatic interactions with the bound ligand. *J. Biol. Inorg. Chem. 2*, 544–552.
56. Dikshit, K. L., Orii, Y., Navani, N., Patel, S., Huang, H. Y., Stark, B. C., and Webster, D. A. (1998) Site-directed mutagenesis of bacterial hemoglobin: the role of glutamine (E7) in oxygen-binding in the distal heme pocket. *Arch. Biochem. Biophys. 349*, 161–166.
57. Dou, Y., Admiraal, S. J., Ikeda-Saito, M., Krzywda, S., Wilkinson, A. J., Li, T., Olson, J. S., Prince, R. C., Pickering, I. J., and George, G. N. (1995) Alteration of axial coordination by protein engineering in myoglobin. Bisimidazole ligation in the His64→Val/Val68→His double mutant. *J. Biol. Chem. 270*, 15993–16001.
58. Weiland, T., Kundu, S., Trent, J., Hoy, J., and Hargrove, M. (2004) Bis-histidyl hexacoordination in hemoglobins facilitates heme reduction kinetics. *J. Am. Chem. Soc. 126*, 11930–11935.
59. Hargrove, M. S., and Olson, J. S. (1996) The stability of holomyoglobin is determined by heme affinity. *Biochemistry 35*, 11310–11318.
60. Aranda, R. T., Cai, H., Worley, C. E., Levin, E. J., Li, R., Olson, J. S., Phillips, G. N., Jr., and Richards, M. P. (2009) Structural analysis of fish versus mammalian hemoglobins: effect of the heme pocket environment on autooxidation and hemin loss. *Proteins 75*, 217–230.
61. Brantley, R. E., Jr., Smerdon, S. J., Wilkinson, A. J., Singleton, E. W., and Olson, J. S. (1993) The mechanism of autooxidation of myoglobin. *J. Biol. Chem. 268*, 6995–7010.